Temporal variations of reference evapotranspiration in Heihe River basin of China

Zhanling Li, Zhanjie Li, Zongxue Xu and Xun Zhou

ABSTRACT

Temporal variations in reference evapotranspiration (ET_o) have profound implications for hydrological processes as well as for agricultural crop performance. The main aim of this study was to analyze the annual, seasonal trends in ET_o in the Heihe River basin. The likely causative meteorological variables for such temporal changes in ET_o were also identified. Results showed that, on a seasonal and annual scale, ET_o for the upper reach showed increasing trends from 1960 to 2010; both increasing and decreasing trends were observed for the middle and lower reaches. In spring, wind speed (WS) and relative humidity (RH) were the most likely causative variables for changes of ET_o for the whole basin; in summer and autumn, maximum temperature (T_{max}) and RH contributed more to the trends in ET_o for the upper reach, and WS contributed more for the middle and lower reaches; in winter, T_{max}, WS and RH contributed more in different locations and in different seasons. From the spatial perspective, WS, RH and T_{max} contributed more to the changes of ET_o in the upper reach; WS was the main likely influence factor in the middle reach, and WS and RH were the probable main factors in the lower reach.

Key words | detrending, Heihe River, Mann–Kendall, Penman–Monteith, reference evapotranspiration

Zhanling Li (corresponding author)
Xun Zhou
School of Water Resources and Environment,
China University of Geosciences,
Beijing 100083,
China
E-mail: *zhanling.li@cugb.edu.cn*

Zhanjie Li
Zongxue Xu
Key Laboratory of Water and Sediment Sciences,
Ministry of Education,
College of Water Sciences,
Beijing Normal University,
Beijing 100875,
China

INTRODUCTION

Evapotranspiration (ET) is an important component of the hydrological cycle, and the record or estimation of it is invaluable in unraveling the aerodynamic and radiative drivers of the hydrological cycle (Roderick *et al.* 2007). The changes in ET are of great interest for water resources planning, irrigation control and agricultural production (Goyal 2004; Sabziparvar *et al.* 2011). Two different aspects of ET have been distinguished: potential evapotranspiration (PET) and actual evapotranspiration (AET). AET, the quantity of water that is actually removed from a surface due to the processes of evaporation and transpiration, is more useful in indicating the effects of climate change and human activity. However, it is often difficult to quantify as it not only requires expensive instrumentation and demands tedious installation and maintenance procedures (Senay *et al.* 2008), but is also affected by the interdependence and the spatial and temporal variability of affecting factors such as solar radiation, air temperature, humidity, wind speed (WS), crop type, variety and environmental conditions (Gervais *et al.* 2012; Tabari *et al.* 2012). Therefore, PET, a maximum value of ET for a saturated surface assuming no control on the water supply, is more commonly used, which is relatively easy to calculate using local meteorological parameters. As an alternative, reference evapotranspiration (ET_o), the ET rate from a hypothetical grass reference crop with specific characteristics, not short of water, is recommended due to its unambiguous definition (Allen *et al.* 1998; Xu *et al.* 2006a; Senay *et al.* 2008; Jhajharia *et al.* 2012).

Exploration of ET changes is currently a very active area of research due to its important role in the hydrological cycle. Both increasing and decreasing trends have been found in ET in different parts of the world. Peterson *et al.* (1995) found Pan Evaporation (Epan) over much of Russia and the United States decreased. Jhajharia *et al.* (2012) reported both seasonal and annual ET_o decreased in

doi: 10.2166/nh.2012.125

northeast India. Burn & Hesch (2007) witnessed a decreasing trend in evaporation in June, July, August, October and the warm season, and an increasing trend in April on the Canadian prairies. In arid and semi-arid regions, monitoring the temporal variations of ET is more important due to its vital role in offering valuable information for agricultural water demand and irrigation practices. In Iran, more than 75% of the country's area is classified as arid or semi-arid. Tabari *et al.* (2012) found that both seasonal and monthly ET_o in most of Iran showed increasing trends. In arid regions of southern Russia, Golubev *et al.* (2001) reported AET showed increasing trends. In Australia, Whetton (2001) concluded that areal ET would most likely increase over most of Australia, while Roderick & Farquhar (2004) detected the Epan decreased at many Australian observing stations. In arid regions of China, it was also found that Epan showed a statistically significant decreasing trend.

As many studies have revealed, changes in ET do not always show orthokinetic responses to temperature change contrary to general expectations (e.g. Chen *et al.* 2006; Xu *et al.* 2006a; Rayner 2007; Bandyopadhyay *et al.* 2009; Liu *et al.* 2010; Wang *et al.* 2011; Jhajharia *et al.* 2012), thus, it is necessary and of great importance to identify which meteorological variable is a likely causative for such a change in ET_o. Such causative meteorological variables have been found to be different across various regions. Jung *et al.* (2010) found that the recent decline of the global land ET trend could be largely explained by increasing soil-moisture limitations, particularly in Africa and Australia. Jhajharia *et al.* (2012) regarded that the main contributions for decreasing seasonal and annual ET_o in northeast India were mainly from the decreased net radiation and WS. Tabari *et al.* (2012) explored that in the arid and semi-arid regions of Iran, the increasing trend of ET_o was most likely due to a significant increase in minimum air temperature, while a decreasing trend of ET_o was mainly caused by a significant decrease in WS. To sum up, the variables of WS (Chen *et al.* 2006; Xu *et al.* 2006a, b; Rayner 2007; Bandyopadhyay *et al.* 2009; Cong *et al.* 2009; Liu *et al.* 2010; Wang *et al.* 2011; Jhajharia *et al.* 2012), relative humidity (RH) (Chattopadhayay & Hulme 1997; Thomas 2000; Bandyopadhyay *et al.* 2009; Wang *et al.* 2011), extreme temperatures (Thomas 2000) and radiation (Chattopadhayay & Hulme 1997; Cohen *et al.* 2002; Wang *et al.* 2011; Jhajharia *et al.* 2012) are all likely causatives for changes in ET_o in terms of the previous studies.

Heihe River basin is located in the arid and semi-arid regions of China. While many studies have been carried out with regard to the trends of ET for basins like Yellow River basin (Liu *et al.* 2010), Yangtze River basin (Xu *et al.* 2006a; Wang *et al.* 2007) Songhua River basin (Gao *et al.* 2006), Haihe River basin (Wang *et al.* 2011), etc., only a few results can be found in the literature for the inland river basin. Water resources in the Heihe River basin are very limited, whereas agriculture there plays an important role by offering both food security and economic security for local and neighboring people. For example, Zhangye region, located in the middle reach of the basin, exports a majority of local agricultural products all over the country. Irrigation is the largest water user in the basin. In agricultural regions that rely on irrigation, investigating the variations of ET is critical not only for managers implementing water-efficient irrigation practices, but also for offering information for regional hydrological processes. In this study, we mainly focus on: (1) estimating ET_o using the Penman–Monteith (PM) method at annual and seasonal temporal scales over 10 stations in Heihe River basin; (2) investigating the trends and quantifying the magnitude of temporal trends in ET_o using the Mann–Kendall (MK) nonparametric test; (3) quantifying the trends in meteorological variables using a linear regression model; and (4) identifying the contributions of trends in meteorological variables to the trends in ET_o using a detrending method over the study area.

STUDY AREA AND DATA

Heihe River basin is the second largest inland river basin in China with a length of 821 km and an area of 142,900 km^2. From the Qilian mountains to the Yingluoxia hydrological station (denoted as H1 station in Figure 1) can be regarded as the upper reach of the basin, and belongs to the cold semi-arid mountain zone dominated by shrubs and trees with an annual mean temperature of less than 2 °C and annual precipitation of 350 mm. From the Yingluoxia station to the Zhengyixia station (denoted as H2 in Figure 1) is regarded as the middle reach, belonging to the mid-stream temperate

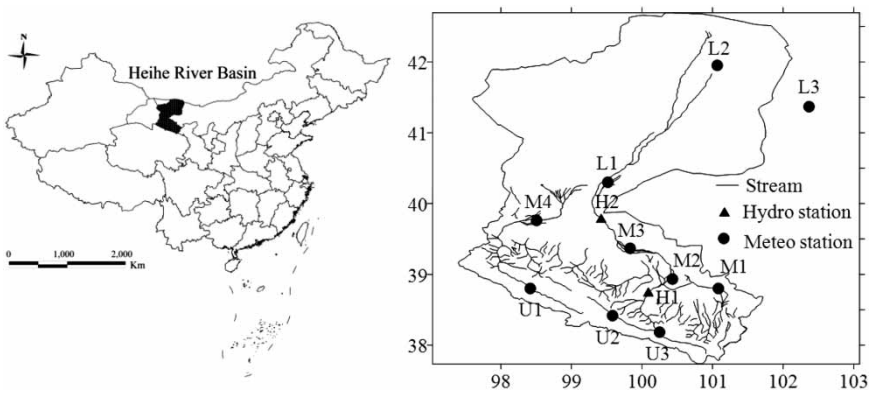

Figure 1 | Location of Heihe River basin and the meteorological stations (in the right chart, *X*-axis indicates longitude (°E), and *Y*-axis indicates latitude (°N)).

zone controlled by cash crops like wheat and corn, with an annual mean temperature less than 6–8 °C and annual precipitation of 140 mm. Finally, from the Zhengyixia station to the north is the lower reach of the basin, pertaining to the downstream warm temperate zone, with an annual mean temperature of 8–10 °C and annual precipitation of only up to 47 mm. For the determination of ET_o, daily maximum and minimum air temperatures (T_{max}, T_{min}), RH, WS, sunshine hour (SH) measured at 10 stations during a period of 51 years (1960–2010) are used. The geographical and meteorological records of the stations are presented in Table 1 and Figure 1. As shown, three stations are in the upper reach (Tuole, Yeniugou and Qilian, denoted as U1, U2 and U3), four in the middle (Shandan, Zhangye, Gaotai and Jiuquan, denoted as M1–M4) and three in the lower reach (Dingxin, Ejinaqi and Guaizihu, denoted as L1–L3). These meteorological data are obtained from the China Meteorological Data Sharing Service System and are of good quality without any missing values through data checking.

METHODS

The Penman–Monteith method

A large number of methods have been developed to estimate ET_o from different climatic variables, e.g. the Blaney–Criddle method, Hargreave's formula, the Penman equation, the Jensen–Hays formula, the modified Penman equation and the PM method (Sammis *et al.* 2011). Among the methods available, the PM method is found to be more consistent over a wider range of climatic conditions than the other equations (López-Urrea *et al.* 2006; Sammis *et al.* 2011),

Table 1 | Basic information of 10 meteorological stations in Heihe River basin

Reach	Station ID	Station name	Latitude (N)	Longitude (E)	Elevation (m a.s.l)	WS (m/s)	T_{mean} (°C)	T_{max} (°C)	T_{min} (°C)	RH (%)	SH (hour)
Upper	U1	Tuole	38°48′	98°25′	3,367	2.2	–2.6	6.7	–10.0	52	2,983
	U2	Yeniugou	38°25′	99°35′	3,320	2.6	–2.9	6.5	–10.2	58	2,686
	U3	Qilian	38°11′	100°15′	2,787	1.9	1.1	10.3	–5.8	54	2,856
Middle	M1	Shandan	38°48′	101°05′	1,764	2.4	6.6	14.8	–0.1	47	2,931
	M2	Zhangye	38°56′	100°26′	1,482	2.0	7.5	15.9	0.5	52	3,085
	M3	Gaotai	39°22′	99°50′	1,332	2.1	7.9	16.0	1.0	54	3,104
	M4	Jiuquan	39°46′	98°29′	1,477	2.2	7.6	15.0	1.1	48	3,061
Lower	L1	Dingxin	40°18′	99°31′	1,177	3.1	8.5	16.6	1.3	45	3,331
	L2	Ejinaqi	41°57′	101°04′	940	3.3	9.0	16.8	1.7	34	3,404
	L3	Guaizihu	41°22′	102°22′	960	4.6	9.2	17.0	2.1	32	3,342

Note: WS (wind speed), T_{mean} (mean air temperature), T_{max} (maximum air temperatures), T_{min} (minimum air temperatures), RH (relative humidity), SH (sunshine hour) are the means of datasets from 1960 to 2010.

therefore it is recommended by the Food and Agricultural Organization as the standard method to determine ET_o for either a short reference crop (similar to clipped grass, 0.12 m tall) or tall reference crop (similar to full-cover alfalfa, 0.5 m tall) (Allen *et al.* 1998). The PM method is physically based and explicitly incorporates both physiological and aerodynamic parameters and will be employed in this study:

$$ET_o = \frac{0.408\Delta(R_n - G) + \gamma \frac{900}{T+273} u_2 (e_s - e_a)}{\Delta + \gamma(1 + 0.34u_2)} \quad (1)$$

where ET_o is the reference evapotranspiration (mm day^{-1}), R_n the net radiation at the crop surface (MJ m^{-2} day^{-1}), G the soil heat flux density (MJ m^{-2} day^{-1}), T air temperature at 2 m height (°C), u_2 WS at 2 m height (m s^{-1}), e_s saturation vapor pressure (kPa), e_a actual vapor pressure (kPa), $e_s - e_a$ saturation vapor pressure deficit (kPa), Δ slope vapor pressure curve (kPa $°C^{-1}$), γ psychrometoic constant (kPa $°C^{-1}$). The geographic location and altitude of the station, and measured meteorological data including daily mean, maximum and minimum temperatures, WS, SH, RH, etc. at the station are needed for the estimation of ET_o, which is introduced in detail in Chapter 3 of FAO Paper 56 (Allen *et al.* 1998).

Temporal trends

The MK test (Mann 1945; Kendall 1975; Li *et al.* 2008; Caloiero *et al.* 2011), one of the popular nonparametric methods for trend analysis, will be used herein. The MK test statistic S is given as follows:

$$S = \sum_{k=1}^{n-1} \sum_{j=k+1}^{n} \mathrm{sgn}(x_j - x_k) \quad (2)$$

where x_j is the data value at time j, n is the length of the dataset and sgn(z) is equal to $+1$, 0, -1, if z is greater than, equal to, or less than zero, respectively. For $n > 10$, the test statistic

$$Z = \begin{cases} \frac{S-1}{\sqrt{\mathrm{Var}(S)}} & \text{if} \quad S > 0 \\ 0 & \text{if} \quad S = 0 \\ \frac{S-1}{\sqrt{\mathrm{Var}(S)}} & \text{if} \quad S < 0 \end{cases} \quad (3)$$

approximately follows a standard normal distribution, in which $\sqrt{\mathrm{Var}(S)}$ is the standard deviation of statistic S. If $|Z| > Z_{(1-\alpha/2)}$, the null hypothesis of no autocorrelation and trend in dataset is rejected, in which $Z_{(1-\alpha/2)}$ is corresponding to the normal distribution with α being the significance level. If the data has a trend, the magnitude of trend can be denoted by trend slope β:

$$\beta = \mathrm{Median}\left(\frac{x_i - x_j}{i - j}\right), \quad \forall\, j < i \quad (4)$$

Detrending method

Detrending, a statistical or mathematical operation of removing trend from the series, is a useful tool for determining the contributions of trends in meteorological variables to trends in ET_o (Xu *et al.* 2006a; Liu *et al.* 2010). Many methods are available for detrending. In this study, the simple linear regression is used to fit the dataset of meteorological variable x_t:

$$\hat{g}_t = \hat{a} + \hat{b}t \quad (5)$$

where $\hat{g}_t$ is the fitted trend at time t, $\hat{a}$ and $\hat{b}$ are the estimated regression constant and the estimated regression coefficient, respectively. Once the trend line has been fitted to the data, one of the options for removing the trend is subtracting the value of the trend line from the original data, that is:

$$y_t = x_t - \hat{g}_t \quad (6)$$

where y_t is the detrended time series. To avoid the negative values for meteorological variables (e.g. WS, RH and SH), instead of $y_t = x_t - \hat{g}_t$, the detrended dataset is currently defined as

$$y_t = x_t - \hat{g}_t + x_1 \quad (7)$$

where x_1 corresponds to the first value of the original time series. After removing the trends in meteorological variables (e.g. WS), the ET_o will be recalculated using the detrended data series (detrended WS dataset) with the other three

original meteorological variables (original T_{max}, T_{min} and RH datasets without detrending), then compared with the original ET_o. The difference between them is regarded as the contribution of the trend by that variable (Xu *et al.* 2006a; Liu *et al.* 2010). In order to quantify the contribution, an evaluating indicator R is constructed:

$$R = \sum_{i=1}^{n} \frac{|ET_o^o i - ET_o^R i|}{ET_o^o i} \quad (8)$$

where ET_o^o and ET_o^R denotes the original and recalculated ET_o obtained from the original and the detrended metrological variables, n is the length of time series. The larger value of R, the greater the contribution of the trend in that variable to the trend in ET_o. $R = 0$ indicates the trend in that variable has no contribution to the trend in ET_o.

RESULTS AND ANALYSIS

Estimations of ET_o over the study area

The four seasons of the study area are defined as: spring (March–May), summer (June–August), autumn (September–November) and winter (December–February). The annual and monthly ET_o obtained through the PM method over 10 stations for the period of 1960–2010 in the study area are presented in Table 2. As shown, the annual ET_o varies from 765 mm in the upper reach to 1,631 mm in the lower reach and is estimated to be 1,178 mm for the whole basin. The monthly ET_o in January and February is around 20–50 mm, and reaches a peak value in June or July, with a range of 160–300 mm for most stations, and afterwards, decreases gradually, reaching about 20 mm in December. The highest ET_o are mainly found in June or July and lowest ET_o are found in December and January. The highest percentage of ET_o occurs in summer, accounting for more than 40% of the total, followed by spring which accounts for 30%, and winter ET_o is the lowest with less than 10% of the total value.

With regard to the spatial distribution of seasonal and annual ET_o in the study area, lower values correspond to the upper reach and higher values to the lower reach. ET_o calculated herein is independent of crop type, crop development and management practices (Allen *et al.* 1998). The only factors affecting ET_o are climatic parameters which provide energy for vaporization and remove water vapor from the evaporating surface. Solar radiation is the largest energy source and is able to change large quantities of liquid water into water vapor. It differs at various latitudes and in different seasons. In general, it is shown to be greater in hot summer than in cold winter. Air temperature controls the rate of ET_o through transferring energy to the crop by

Table 2 | Monthly and annual ET_o obtained from Penman–Monteith method during the period of 1960–2010 in Heihe River basin (mm)

Station ID/Reach	JAN	FEB	MAR	APR	MAY	JUN	JUL	AUG	SEP	OCT	NOV	DEC	Annual
U1	16	27	53	80	101	107	113	103	73	48	23	15	757
U2	21	30	51	74	91	94	97	88	63	46	28	21	702
U3	22	33	60	88	112	117	116	106	77	55	31	19	838
M1	27	39	76	121	160	170	168	158	110	76	43	28	1,175
M2	24	39	77	123	158	165	166	149	101	66	36	23	1,125
M3	22	37	78	125	159	167	167	148	100	65	33	19	1,119
M4	24	38	78	130	164	170	166	152	109	75	41	23	1,170
L1	29	45	89	142	189	200	201	178	126	86	48	31	1,362
L2	23	42	94	165	235	261	260	223	155	95	48	24	1,625
L3	29	50	109	188	267	300	301	265	186	118	61	32	1,906
Upper	19	30	55	81	101	106	108	99	71	50	27	18	765
Middle	24	38	77	125	160	168	167	152	105	70	38	23	1,147
Lower	27	46	97	165	230	254	254	222	156	100	52	29	1,631

the heat of the surrounding air. WS and RH impact ET_o through affecting the process of water vapor removal. The greater WS, the greater the driving force for water vapor removal. Compared with those for the upper reach, T_{mean}, T_{max}, and T_{min} for the middle reach increase by 7–9 °C, and T_{mean}, T_{max}, and T_{min} for the lower reach increase by 9–10 °C, the average WS increase by 64%, and RH decrease by 32%. These changes in climatic parameters would cause increases in ET_o in the middle and lower reaches.

The mean annual ET_o reach 1,625 and 1,906 mm at U2 and U3 stations in the lower reach. The mean annual precipitation during the period of 1960 to 2010 is about 35 and 45 mm for U2 and U3 stations, respectively, based on the records from the meteorological stations. This implies that the mean annual ET_o in the lower reach is more than 42 times greater than the mean annual precipitation. Thus, the lower reach is usually confronted with severe water deficits.

Temporal trends of ET_o over the study area

Results from the MK test for seasonal and annual ET_o for each station are presented in Table 3, together with the magnitude of trend and the significance level. On the annual scale, ET_o data for the upper reach show increasing trends during the past 51 years, with two out of three showing increasing tendency deemed significant at the >95% confidence interval (CI). Both increasing and decreasing trends in ET_o were observed for the middle reach, while most of the trends are not significant at >90% CI. For the lower reach, ET_o at L1 station shows a slightly increasing trend, and changes in the opposite way for the other two stations, with significant decreasing at L2 station, and significant increasing at L3 station (at >95% CI).

On the seasonal scales, all ET_o for the upper reach show increasing trends, and 42% (five series of 12) of the increasing tendency are significant at >95% CI. ET_o at U1 station increases most for all seasons compared with other stations. For the middle reach, both increasing and decreasing trends in ET_o are found with the greatest increase occurring in summer ET_o at M2 station and greatest decrease occurring in summer ET_o at M3 station. However, most of the trends are not significant at >90% CI. For the lower reach, similar to the annual scale, slightly increasing trends are found in spring, summer and autumn ET_o for L1 station. Decreasing ET_o is found for L2 station, and increasing ET_o is found for L3 station for all seasons. Both L2 and L3 stations are located in the arid climatic zone, and geographically close to the Badanjilin Desert, with the main characteristics of being dry, hot, windy and short of rain. In such a hot and dry region, the ET demand is becoming high due to the dryness of the air and the amount of energy available as direct solar radiation and latent heat. The quite different trends in ET_o for the other two stations are probably attributed to the different tendency in meteorological conditions especially in

Table 3 | Trends for seasonal and annual ET_o for each station during the period of 1960–2010

	Spring		Summer		Autumn		Winter		Annual	
Station ID	***T***	***β***	***T***	***β***	***T***	***β***	***T***	***β***	***T***	***β***
U1	↑***	0.53	↑**	0.50	↑***	0.43	↑***	0.50	↑***	1.87
U2	–	0.10	–	0.17	–	0.04	–	0.09	–	0.22
U3	–	0.06	–	0.08	↑*	0.25	–	0.12	↑$^{+}$	0.52
M1	–	−0.10	–	−0.51	–	−0.03	↑*	0.27	–	−0.27
M2	–	−0.02	–	0.33	–	−0.06	–	0.09	–	0.25
M3	↓$^{+}$	−0.53	↓*	−1.05	↓**	−0.59	–	−0.20	↓**	−2.69
M4	–	−0.11	–	0.20	–	−0.26	–	−0.05	–	0.17
L1	–	0.38	–	0.08	–	0.10	–	−0.04	–	0.50
L2	↓*	−0.73	↓**	−1.63	↓*	−0.53	–	0.02	↓**	−2.75
L3	↑***	1.85	↑***	2.94	↑***	1.42	↑**	0.48	↑***	6.60

Note: '***,**,*,+' means the significance level of 0.001, 0.01, 0.05 and 0.1.

WS. Under arid conditions, the drier the atmosphere, the larger the effect of WS on ET_o. Decreasing WS at L2 station may result in decreasing the ET_o since WS is the most likely causative variable for changes of ET_o at L2 station in the four seasons (Tables 4 and 5). Increasing WS and decreasing RH at L3 station would cause an increase in ET_o in the

Table 4 | Slopes of linear trends in five meteorological variables in Heihe River basin

Variable	Season	U1	U2	U3	M1	M2	M3	M4	L1	L2	L3
WS (m/s)	Spring	0.011	0.000	−0.005	−0.013	−0.018	−0.025	−0.009	−0.010	−0.029	0.011
	Summer	0.007	−0.002	−0.007	−0.011	−0.010	−0.026	−0.007	−0.010	−0.035	0.011
	Autumn	0.009	0.000	−0.001	−0.008	−0.010	−0.020	−0.006	−0.011	−0.026	0.014
	Winter	0.013	−0.002	−0.002	−0.008	−0.007	−0.017	−0.004	−0.016	−0.020	0.010
T_{max} (°C)	Spring	0.016	0.010	0.004	0.014	0.024	0.021	0.016	0.025	0.019	0.012
	Summer	0.027	0.024	0.014	0.015	0.029	0.022	0.026	0.024	0.022	0.023
	Autumn	0.037	0.029	0.028	0.030	0.035	0.033	0.029	0.036	0.028	0.027
	Winter	0.048	0.038	0.037	0.044	0.039	0.033	0.031	0.034	0.048	0.025
T_{min} (°C)	Spring	0.009	0.037	0.028	0.045	0.036	0.027	0.026	0.035	0.059	0.067
	Summer	0.032	0.037	0.036	0.041	0.049	0.022	0.025	0.032	0.056	0.069
	Autumn	0.035	0.036	0.036	0.067	0.035	0.015	0.024	0.029	0.075	0.083
	Winter	0.045	0.056	0.059	0.112	0.057	0.047	0.036	0.042	0.100	0.078
RH (%)	Spring	−0.062	0.063	0.000	−0.043	−0.083	−0.031	0.009	−0.126	−0.057	−0.099
	Summer	0.002	0.024	−0.053	0.021	−0.075	−0.012	−0.026	−0.073	−0.087	−0.145
	Autumn	−0.056	0.076	−0.045	−0.058	−0.001	0.064	0.094	−0.054	−0.015	−0.048
	Winter	−0.110	0.076	0.050	−0.171	−0.018	0.062	0.032	−0.030	−0.049	−0.005
SH (hour)	Spring	0.007	0.003	−0.002	−0.002	0.001	0.010	0.007	−0.001	−0.002	0.013
	Summer	−0.001	−0.006	−0.011	−0.010	0.002	−0.005	−0.003	−0.001	−0.004	0.009
	Autumn	0.002	0.002	−0.002	−0.008	−0.001	−0.011	−0.008	−0.007	−0.006	0.008
	Winter	0.002	−0.001	−0.010	−0.015	−0.012	−0.016	−0.002	−0.002	−0.010	0.002

Table 5 | Values of evaluating indicator *R* for identifying the contributions of trends in meteorological variables to trends in ET_o

Season	Variable	U1	U2	U3	M1	M2	M3	M4	L1	L2	L3
Spring	WS	**0.83**	0.09	**0.58**	**1.77**	**2.62**	**3.69**	**1.23**	**1.14**	**3.95**	**1.02**
	T_{max}	0.73	0.46	0.18	0.30	0.81	0.71	0.59	0.94	0.71	0.50
	T_{min}	0.18	0.68	0.46	0.60	0.45	0.34	0.35	0.37	0.61	0.70
	RH	**0.88**	**0.88**	0.08	0.38	0.85	0.40	0.03	**1.52**	0.59	**1.21**
	SH	0.27	0.15	0.01	0.00	0.12	0.36	0.23	0.01	0.02	0.19
Summer	WS	0.35	0.06	0.44	**1.28**	**1.28**	**3.15**	**0.96**	**1.37**	**5.09**	**1.19**
	T_{max}	**0.83**	**0.62**	0.38	0.36	**0.70**	0.53	**0.63**	0.63	0.55	0.60
	T_{min}	0.47	**0.60**	0.50	0.40	0.47	0.25	0.27	0.28	0.36	0.46
	RH	0.02	0.41	**0.52**	0.19	0.61	0.10	0.23	**0.64**	0.73	**1.52**
	SH	0.03	0.30	**0.52**	0.37	0.10	0.21	0.14	0.02	0.09	0.15
Autumn	WS	**1.21**	0.02	0.07	**1.36**	**1.57**	**3.23**	**0.98**	**1.56**	**4.34**	**1.55**
	T_{max}	**1.23**	**1.00**	**0.81**	0.80	0.88	0.76	0.74	**1.08**	0.91	0.91
	T_{min}	0.56	0.67	0.51	0.66	0.45	0.12	0.19	0.26	0.65	0.83
	RH	0.29	**1.24**	0.48	0.49	0.10	0.73	**1.10**	0.64	0.24	0.58
	SH	0.02	0.02	0.12	0.28	0.12	0.54	**1.45**	0.31	0.11	0.04
Winter	WS	**4.62**	0.47	0.67	1.89	**2.02**	**4.43**	**1.10**	**2.25**	**4.22**	**1.33**
	T_{max}	**3.04**	**2.24**	**2.07**	**2.19**	**2.00**	1.75	**1.63**	**1.83**	**2.51**	**1.49**
	T_{min}	1.06	0.82	**1.01**	1.60	0.86	0.79	0.70	0.60	**1.47**	**1.34**
	RH	1.76	**1.56**	0.79	**2.93**	0.49	1.07	0.53	0.65	0.95	0.19
	SH	0.35	0.02	0.20	0.14	0.18	0.22	0.50	0.01	0.07	0.01

spring and summer seasons. Increasing WS in autumn and increasing T_{max} and T_{min} in winter at L3 station may result in an increasing ET_o in autumn and winter seasons.

Temporal trends in meteorological variables

In order to indentify the contributions of trends in meteorological variables to trends in ET_o, linear regression detrending method is employed for the time series of meteorological variables including WS, T_{max}, T_{min}, RH and SH on monthly temporal scales. The original and detrended time series on seasonal scales are aggregated from the monthly results obtained above.

Figure 2, simply taking L2 station and summer as an example due to the limited space, shows the original and detrended time series of meteorological variables, together with their linear trend lines and linear regression models. Linear trends in meteorological variables in spring, autumn and winter seasons for L2 station are shown in Table 4. As shown, WS, RH and SH at this station show decreasing

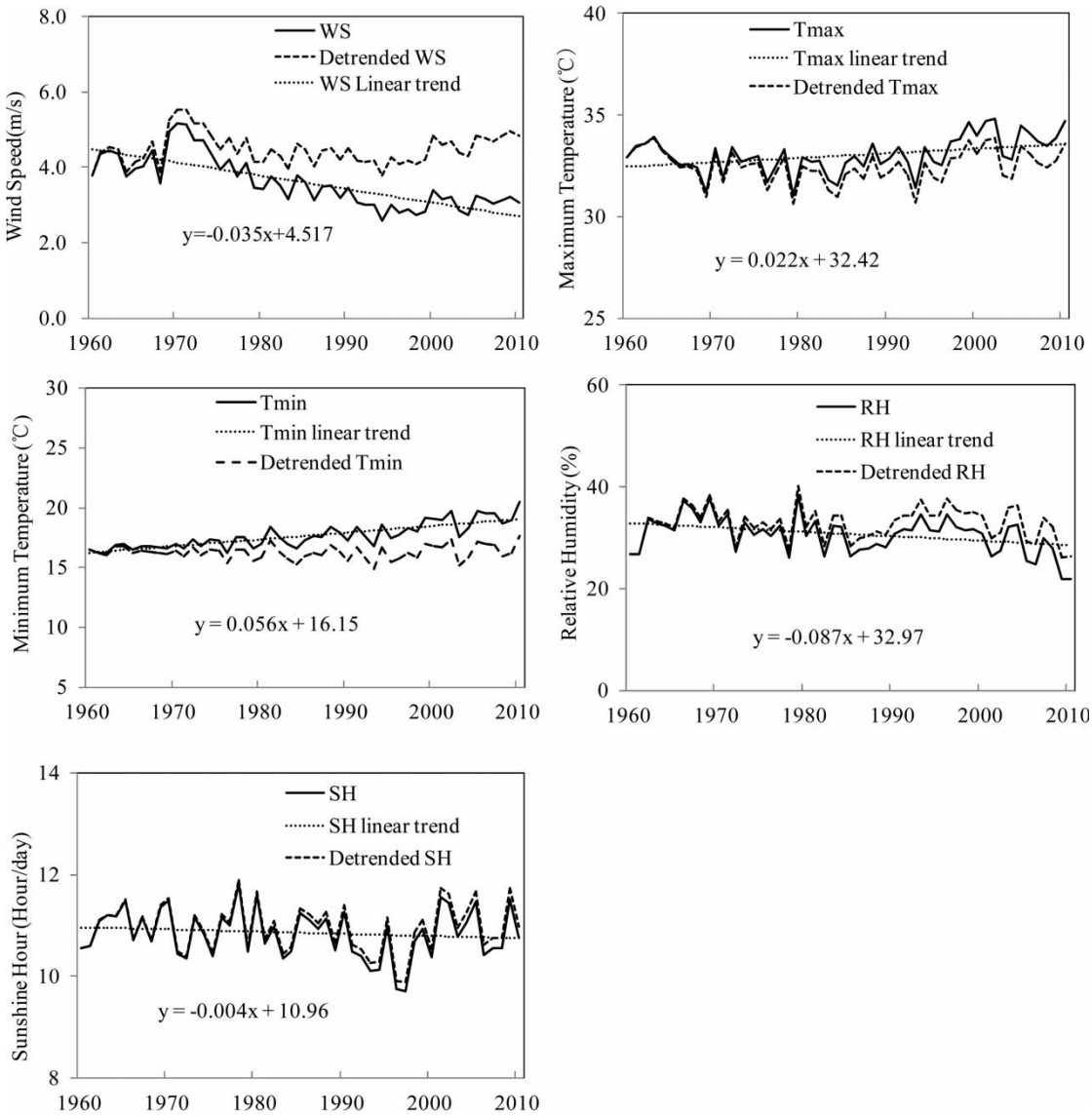

Figure 2 | The original and detrended meteorological variables for Ejinaqi (L2) station in summer using linear regression detrending method.

trends in all seasons. The highest decreasing magnitude appears in summer for WS and RH, and appears in winter for SH. T_{max} and T_{min} at L2 station present increasing trends in all seasons, with the highest increasing magnitudes occurring in winter. The increasing magnitudes for T_{min} are greater than those for T_{max} in all seasons. ET_o at L2 station show significant decreasing trends on seasonal scale except for winter season in terms of the above analysis (Table 3). It implies that, the increasing temperature cannot give a satisfactory explanation to the decreasing ET_o at this station due to the complicated interaction of many other influencing factors involved, which also has been proved in many previous studies and over many arid areas (e.g. Chattopadhayay & Hulme 1997; Roderick *et al.* 2007; Tabari *et al.* 2012).

Returning to Table 4, for the upper reach, increasing trends at U1 station are found in WS, T_{max} and T_{min}, increasing trends at U2 station in T_{max}, T_{min} and RH, increasing trends at U3 station in T_{max} and T_{min} for all seasons. Both decreasing and increasing trends for SH are detected in different seasons for the upper reach. For the middle reach, all stations are characterized by the decreasing trends in WS, increasing trends in T_{max} and T_{min}, and both decreasing and increasing trends in RH and SH. For the lower reach, decreasing trends are detected in WS, RH and SH, and increasing trends are detected in T_{max} and T_{min} at L1 station for all seasons. Increasing trends are found in WS, T_{max}, T_{min}, SH and decreasing trends in RH at L3 station for all seasons. For the whole basin, most of the increasing magnitudes for T_{min} are higher than those for T_{max} in four seasons, which is consistent with the global pattern in the last decades (Zhang *et al.* 2004; Song *et al.* 2010) and the increasing magnitudes in T_{max} and T_{min} in winter are higher than those in other seasons.

Additionally, all stations (100%) are characterized by increasing T_{max} and T_{min}, 60–70% of stations are characterized by decreasing RH, and 70–80% of stations are characterized by decreasing WS, thus both increasing and decreasing trends are found in ET_o for the basin as a result of their combined effects.

Identification of contributions of trends in meteorological variables to trends in ET_o

Figure 3, taking L2 station and taking summer as an example, shows the original and recalculated ET_o using the original and detrended meteorological datasets based

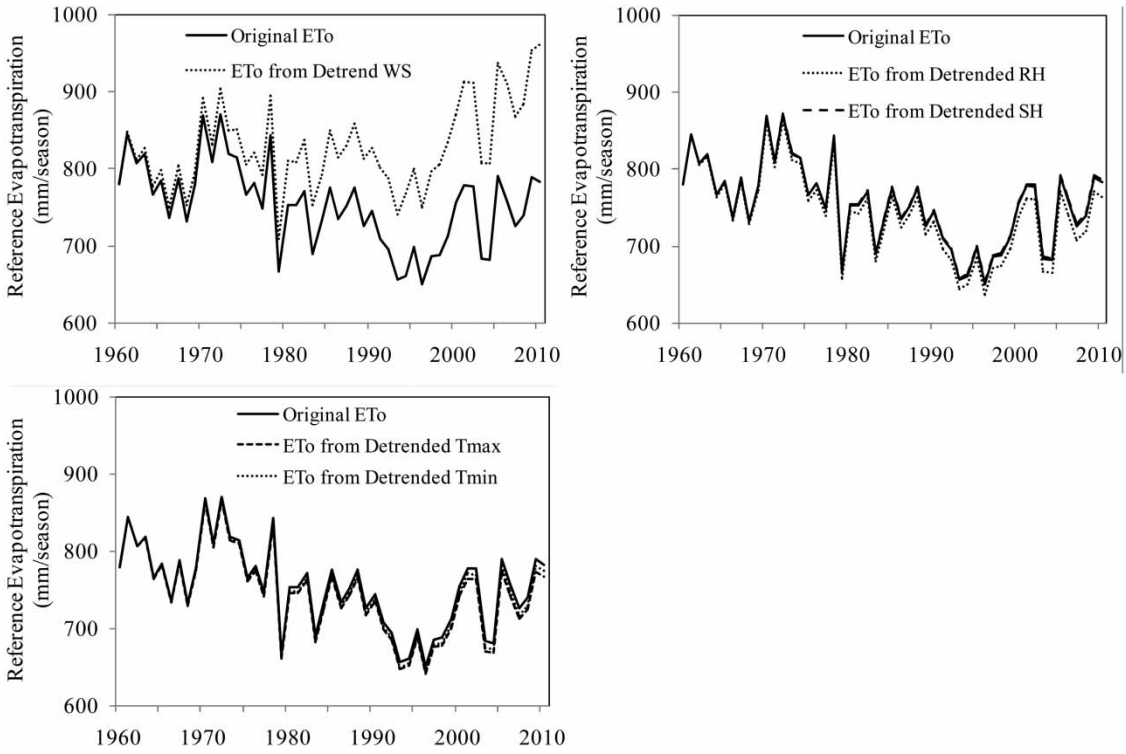

Figure 3 | The original and recalculated summer ET_o for Ejinaqi (L2) station with detrended wind speed, relative humidity and sunshine hours and maximum and minimum temperatures.

on the PM method. The largest difference between the original ET_o and the recalculated ET_o from detrended WS is found in spring, summer and autumn seasons, which implies that trends in WS have the greatest contributions to the trend in ET_o at L2 station for the three seasons. That is, the decreasing trends in ET_o in spring, summer and autumn seasons (Table 3) could be explained largely by the decreasing trends in WS (Table 4). The WS in winter also presents a decreasing trend although with the smallest decline magnitude compared with those in the other seasons (Table 4), while ET_o in winter shows an opposite increasing trend (Table 3) which can be explained by not only WS, but also T_{max} and T_{min} dominating the trend in winter ET_o for this station. This conclusion also can be drawn from Table 5 (great values of R for not only WS, but T_{max} and T_{min}).

Table 5 presents the values of evaluating indicator R for all meteorological variables on seasonal scales. All values are greater than zero, indicating that the trends in all variables have more or less effects on trends in ET_o. The greater the value of R, the greater contribution of the trend in that variable to the trend in ET_o. The greater values of R are in bold type in Table 5 for a better visualization and to summarize the most likely causative meteorological variables for each station in Table 6.

In spring, WS and RH are the most likely causative meteorological variables for changes of trend in ET_o for the whole basin. In hot and dry area and conditions, the humidity of the air is low and much water vapor can be stored in the air. Wind may promote the transport of water allowing more water vapor to be taken up. With the increasing WS, the air would be continuously replaced with drier air, and the driving force for water vapor removal and the ET would increase. Therefore, increasing WS and decreasing RH at U1 and L3 station in the Heihe River basin would lead to the significantly increasing trends in ET_o; decreasing WS at M1–M4 and L2 stations results in decreasing ET_o; decreasing WS at L1 station counterbalances the effects of decreasing RH, resulting in a slightly increasing trend in ET_o. In summer and autumn, T_{max} and RH contribute more to the trends in ET_o for the upper reach, while WS contributes most for the middle and lower reaches. In winter, more meteorological variables including WS, T_{max} and RH are detected to be responsible for trends in ET_o in different locations and in different seasons. From the spatial perspective, WS, RH and T_{max} contribute more to the changes of ET_o in the upper reach; WS is the main likely influencing factor on the trends of ET_o in the middle reach, and WS and RH are the probable main factors in the lower reach.

These results are consistent with the findings from many previous studies carried out in arid or semi-arid regions. Tabari *et al.* (2012) found that in arid and semi-arid regions of Iran, the increasing trend of ET_o was

Table 6 | The likely causative meteorological variables for changes of ET_o in Heihe River basin

Station ID	Spring	Summer	Autumn	Winter
U1	RH(−0.54), WS(0.61)	T_{max}(0.74)	T_{max}(0.61), WS(0.77)	WS(0.87), T_{max}(0.77)
U2	RH(−0.63)	T_{max}(0.72), T_{min}(0.17)	RH(−0.8), T_{max}(0.62)	T_{max}(0.66), RH(−0.81)
U3	WS(0.51)	RH(−0.87), SH(0.30)	T_{max}(0.56)	T_{max}(0.65), T_{min}(0.60)
M1	WS(0.40)	WS(0.60)	WS(0.40)	RH(−0.65), T_{max}(0.81)
M2	WS(0.50)	WS(0.65), T_{max}(0.61)	WS(0.64)	WS(0.56,) T_{max}(0.51)
M3	WS(0.78)	WS(0.79)	WS(0.86)	WS(0.75)
M4	WS(0.64)	WS(0.55), T_{max}(0.51)	SH(0.29), RH(−0.69), WS(0.71)	T_{max}(0.56), WS(0.62)
L1	RH(−0.76), WS(0.70)	WS(0.75), RH(−0.72)	WS(0.66), T_{max}(0.31)	WS(0.41), T_{max}(0.51)
L2	WS(0.67)	WS(0.77)	WS(0.76)	WS(0.53), T_{max}(0.44), T_{min}(0.41)
L3	RH(−0.77), WS(0.50)	RH(−0.82), WS(0.66)	WS(0.70)	T_{max}(0.60), T_{min}(0.84), WS(0.62)

Note: Values in the brackets are the correlation coefficients between ET_o and the detected meteorological variable using the Spearman method.

most likely due to a significant increase in T_{min}, while a decreasing trend in ET_o was mainly caused by a significant decrease in WS; Thomas (2000) concluded that WS was the variable most strongly associated with ET_o changes in the arid regions of northwest of China. Chen *et al.* (2006) found that the decreasing WS had more influence on the decreasing ET_o in the Tibetan Plateau in China, and Wang *et al.* (2011) reported that the WS and RH were generally recognized as the main driving forces for the decreasing trends in ET_o in the plain and the mountain areas of the Haihe River basin in China.

To test the accuracy and reliability of the most likely causative meteorological variables we derived, a further investigation was carried out on the relationship between ET_o and meteorological variables (WS, T_{mean}, T_{max}, T_{min}, RH and SH) through calculating their correlation coefficients using the Spearman method. The main results of correlation coefficients are given in the brackets in Table 6. As can be seen, the correlations between ET_o and the detected variables are relatively high, with 37% of the coefficients (absolute values) exceeding 0.70, and 66% exceeding 0.60, suggesting that most of the detected variables have strong correlations with ET_o and therefore changes of the detected variables can be used to explain the trends in ET_o to a large extent.

There are large areas of irrigation in the middle reach of the basin and a large volume of water is used in agriculture. In recent years, less and less water flows to the lower reach, leading to the reducing of areas of vegetations and oasis, and aggravating desertification. Regional climate change and human activity (e.g. modifications of agriculture distribution and water allocation) have greatly changed the local meteorological conditions and accordingly affect the trends in ET_o. Understating the variations of ET_o in different locations and in different seasons is thus of great importance for recognizing the local hydrological processes, and more important, has meaningful indications for irrigation practice in the middle reach as well as for the protection and construction of oases in the lower reach. Since there is low vegetation coverage and serious desertification in the lower reach, the calculated ET_o based on a hypothetical reference crop may differ with the AET which reflects the actual processes of evaporation and transpiration, therefore, investigations of AET in the study area will be pursued in future analysis based on remote sensing data.

CONCLUSIONS

Heihe River basin is the second largest inland river basin in the arid and semi-arid northwestern region of China, where water resources are very limited and PET is very high. Investigation of variations in trends of ET_o in the Heihe River basin is critical for offering valuable information for regional hydrological and water resource management. ET_o over 10 stations for the basin from 1960 to 2010 were estimated by employing the PM method. The temporal trends in ET_o and in meteorological variables were detected with the MK test and linear trend method. Through detrending the meteorological variables and calculating the correlation coefficients between ET_o and the meteorological variables, the most likely causative meteorological variables for temporal changes of ET_o were also identified. Results showed the following. (1) On both a seasonal and annual scale, increasing trends in ET_o were found for the upper reach; both increasing and decreasing trends in ET_o were found for the middle and lower reaches. (2) Increasing trends were found in T_{max} and T_{min} for the upper reach. Decreasing trends in WS, increasing trends in T_{max} and T_{min}, and both decreasing and increasing trends in RH and SH were found for the middle reach. For the lower reach, increasing trends were observed in T_{max} and T_{min}, decreasing trends in RH, and both increasing and decreasing trends in WS and SH. (3) Solar radiation and air temperature are the main driving forces for the vaporization of water in ET_o, and WS and RH mostly determine the process of vapor removal. In spring, WS and RH were the most likely causative meteorological variables for changes of ET_o for the basin.

In summer and autumn, T_{max} and RH contributed more to the trends in ET_o for the upper reach, while WS contributed most for the middle and lower reaches. In winter, more meteorological variables including WS, T_{max} and RH were detected to be responsible for trends in ET_o in different locations. From the spatial perspective, changes of WS, RH and T_{max} caused ET_o increases in the upper reach; WS contributed most to

both increasing and decreasing trends in ET_o in the middle reach, and WS and RH were the main likely influencing factors in the lower reach.

ACKNOWLEDGEMENTS

This study is supported by NSFC (No. 41101038), the Fundamental Research Funds for the Central Universities (No. 2652012082), and the Major Research Plan of National Natural Science Foundation of China (No. 91125015). The referees comments are gratefully acknowledged.

REFERENCES

Allen, R. G., Pereira, L. S., Raes, D. & Smith, M. 1998 Crop evapotranspiration–guidelines for computing crop water requirements. FAO Irrigation and Drainage Paper 56. Food and Agricultural Organization of the United Nations, Rome, Italy.

Bandyopadhyay, A., Bhadra, A., Raghuwanshi, N. S. & Singh, R. 2009 Temporal trends in estimates of reference evapotranspiration over India. *Journal of Hydrologic Engineering* **14**, 508–515.

Burn, D. H. & Hesch, N. M. 2007 Trends in evaporation for the Canadian Prairies. *Journal of Hydrology* **336**, 61–73.

Caloiero, T., Coscarelli, R., Ferraric, E. & Mancinia, M. 2011 Trend detection of annual and seasonal rainfall in Calabria (Southern Italy). *International Journal of Climatology* **31**, 44–56.

Chattopadhayay, N. & Hulme, M. 1997 Evaporation and potential evapotranspiration in India under conditions of recent and future climate change. *Agricultural Forest Meteorology* **87**, 55–73.

Chen, S. B., Liu, Y. F. & Thomas, A. 2006 Climatic change on the Tibetan Plateau: potential evapotranspiration trends from 1961–2000. *Climatic Change* **76**, 291–319.

Cohen, S., Ianetz, A. & Stanhill, G. 2002 Evaporative climate changes at Bet Dagan, Israel, 1964–1998. *Agricultural and Forest Meteorology* **111**, 83–91.

Cong, Z. T., Yang, D. W. & Ni, G. H. 2009 Does evaporation paradox exist in China? *Hydrology Earth System Sciences* **13**, 357–366.

Gao, G., Chen, D. L., Ren, G. Y., Chen, Y. & Liao, Y. M. 2006 Spatial and temporal variations and controlling factors of potential evapotranspiration in China: 1956–2000. *Journal of Geographical Sciences* **16**, 3–12.

Gervais, M., Mkhabela, M., Bullock, P., Raddatz, R. & Finlay, G. 2012 Comparison of standard and actual crop evapotranspiration estimates derived from different evapotranspiration methods on the Canadian Prairies. *Hydrological Processes* **26**, 1467–1477.

Golubev, V. S., Lawrimore, J. H., Groisman, P. Ya., Speranskaya, N. A., Zhuravin, S. A., Menne, M. J., Peterson, T. C. & Malone, R. W. 2001 Evaporation change over the contiguous United States and the former USSR: a reassessment. *Geophysical Research Letters* **28**, 2665–2668.

Goyal, R. K. 2004 Sensitivity of evapotranspiration to global warming: a case study of arid zone of Rajasthan (India). *Agricultural Water Management* **69**, 1–11.

Jhajharia, D., Dinpashoh, Y., Kahya, E., Singh, V. P. & Fakheri-Fard, A. 2012 Trends in reference evapotranspiration in the humid region of northeast India. *Hydrological Processes* **26**, 421–435.

Jung, M., Reichstein, M., Ciais, P., Seneviratne, S., Sheffield, J., Goulden, M. L., Bonan, G., Cescatti, A., Chen, J., Jeu, R., Johannes Dolman, A., Eugster, W., Gerten, D., Gianelle, D., Gobron, N., Heink, J., Kimball, J., Law, B. E., Montagnani, L., Mu, Q., Mueller, B., Oleson, K., Papale, D., Richardson, A. D., Roupsard, O., Running, S., Tomelleri, E., Viovy, N., Weber, U., Williams, C., Wood, E., Zaehle, S. & Zhang, K. 2010 Recent decline in the global land evapotranspiration trend due to limited moisture supply. *Nature* **467**, 951–954.

Kendall, M. G. 1975 *Rank correlation methods*. Griffin, London, UK.

Li, Z. L., Xu, Z. X., Li, J. Y. & Li, Z. J. 2008 Shift trend and step changes for runoff time series in the Shiyang River basin, northwest China. *Hydrological Processes* **22**, 4639–4646.

Liu, Q., Yang, Z., Cui, B. & Sun, T. 2010 The temporal trends of reference evapotranspiration and its sensitivity to key meteorological variables in the Yellow River Basin, China. *Hydrological Processes* **24**, 2171–2181.

López-Urrea, R., Mart'ın de Santa Olalla, F., Fabeiro, C. & Moratalla, A. 2006 An evaluation of two hourly reference evapotranspiration equations for semiarid conditions. *Agricultural Water Management* **86**, 277–282.

Mann, H. B. 1945 NonparamET0ic tests against trend. *EconomET0ica* **13**, 245–259.

Peterson, T., Golubev, V. & Groisman, P. 1995 Evaporation losing its strength. *Nature (London)* **377**, 687–688.

Rayner, D. P. 2007 Wind run changes: the dominant factor affecting pan evaporation trends in Australia. *Journal of Climate* **20**, 3379–3394.

Roderick, M. L. & Farquhar, G. D. 2004 Changes in Australian pan evaporation from 1970 to 2002. *International Journal of Climatology* **24**, 1077–1090.

Roderick, M. L., Rotstayn, L. D., Farquhar, G. D. & Hobbins, M. T. 2007 On the attribution of changing pan evaporation. *Geophysical Research Letters* **34**, L17403.

Sabziparvar, A. A., Mirmasoudi, S. H., Tabari, H., Nazemosadat, M. J. & Maryanaji, Z. 2011 ENSO teleconnection impacts on reference evapotranspiration variability in some warm climates of Iran. *International Journal of Climatology* **31**, 1710–1723.

Sammis, T. W., Wang, J. & Miller, D. R. 2011 The Transition of the Blaney-Criddle Formula to the Penman-Monteith Equation in

the Western United States. *Journal of Service Climatology* **5**, 1–11.

Senay, G. B., Verdin, J. P., Lietzow, R. & Melesse, A. M. 2008 Global daily reference evapotranspiration modeling and evaluation. *Journal of the American Water Resources Association* **44**, 969–979.

Song, Z. W., Zhang, H. L., Snyder, R. L., Anderson, F. E. & Chen, F. 2010 Distribution and trends in reference evapotranspiration in the North China Plain. *Journal of Irrigation and Drainage Engineering* **136**, 240–247.

Tabari, H., Aeini, A., Hosseinzadeh Talaee, P. & Shifteh Some'e, B. 2012 Spatial distribution and temporal variation of reference evapotranspiration in arid and semi-arid regions of Iran. *Hydrological Processes* **26**, 500–512.

Thomas, A. 2000 Spatial and temporal characteristics of potential evapotranspiration trends over China. *International Journal of Climatology* **20**, 381–396.

Wang, Y., Jiang, T., Bothe, O. & Fraedrich, K. 2007 Changes of pan evaporation and reference evapotranspiration in the Yangtze River basin. *Theoretical and Applied Climatology* **90**, 13–23.

Wang, W., Peng, S., Yang, T., Shao, Q., Xu, J. & Xing, W. 2011 Spatial and temporal characteristics of reference evapotranspiration trends in the Haihe River basin, China. *Journal of Hydrologic Engineering* **16**, 239–252.

Whetton, P. 2001 *Climate projections for Australia*. CSIRO Marine and Atmospheric Research, Melbourne, Australia, 8 pp.

Xu, C.-Y., Gong, L. B., Jiang, T., Chen, D. L. & Singh, V. P. 2006a Analysis of spatial distribution and temporal trend of reference evapotranspiration and pan evaporation in Changjiang (Yangtze River) catchment. *Journal of Hydrology* **327**, 81–93.

Xu, M., Chang, C. P., Fu, C. B., Qi, Y., Robock, A., Robinson, D. & Zhang, H. M. 2006b Steady decline of East Asian Monsoon winds, 1969–2000: evidence from direct ground measurements of wind speed. *Journal of Geophysical Research* **111**, D24111.

Zhang, Y., Qin, B. & Chen, W. 2004 Analysis of 40 year records of solar radiation in Shanghai, Nanjing and Hangzhou in Eastern China. *Theoretical and Applied Climatology* **78**, 217–227.

First received 14 September 2011; accepted in revised form 15 June 2012. Available online 6 November 2012